CLNS 04/1886, CLEO 04-10, CLEO CONF 04-05, ICHEP04 ABS10-0761

Photon Transitions in $\psi(2S)$ Decays to $\chi_{cJ}(1P)$ and $\eta_c(1S)^*$

S. B. Athar,[1] P. Avery,[1] L. Breva-Newell,[1] R. Patel,[1] V. Potlia,[1] H. Stoeck,[1] J. Yelton,[1] P. Rubin,[2] B. I. Eisenstein,[3] G. D. Gollin,[3] I. Karliner,[3] D. Kim,[3] N. Lowrey,[3] P. Naik,[3] C. Sedlack,[3] M. Selen,[3] J. J. Thaler,[3] J. Williams,[3] J. Wiss,[3] K. W. Edwards,[4] D. Besson,[5] K. Y. Gao,[6] D. T. Gong,[6] Y. Kubota,[6] B.W. Lang,[6] S. Z. Li,[6] R. Poling,[6] A. W. Scott,[6] A. Smith,[6] C. J. Stepaniak,[6] J. Urheim,[6] Z. Metreveli,[7] K. K. Seth,[7] A. Tomaradze,[7] P. Zweber,[7] J. Ernst,[8] A. H. Mahmood,[8] H. Severini,[9] D. M. Asner,[10] S. A. Dytman,[10] S. Mehrabyan,[10] J. A. Mueller,[10] V. Savinov,[10] Z. Li,[11] A. Lopez,[11] H. Mendez,[11] J. Ramirez,[11] G. S. Huang,[12] D. H. Miller,[12] V. Pavlunin,[12] B. Sanghi,[12] E. I. Shibata,[12] I. P. J. Shipsey,[12] G. S. Adams,[13] M. Chasse,[13] M. Cravey,[13] J. P. Cummings,[13] I. Danko,[13] J. Napolitano,[13] D. Cronin-Hennessy,[14] C. S. Park,[14] W. Park,[14] J. B. Thayer,[14] E. H. Thorndike,[14] T. E. Coan,[15] Y. S. Gao,[15] F. Liu,[15] M. Artuso,[16] C. Boulahouache,[16] S. Blusk,[16] J. Butt,[16] E. Dambasuren,[16] O. Dorjkhaidav,[16] N. Menaa,[16] R. Mountain,[16] H. Muramatsu,[16] R. Nandakumar,[16] R. Redjimi,[16] R. Sia,[16] T. Skwarnicki,[16] S. Stone,[16] J. C. Wang,[16] K. Zhang,[16] S. E. Csorna,[17] G. Bonvicini,[18] D. Cinabro,[18] M. Dubrovin,[18] R. A. Briere,[19] G. P. Chen,[19] T. Ferguson,[19] G. Tatishvili,[19] H. Vogel,[19] M. E. Watkins,[19] N. E. Adam,[20] J. P. Alexander,[20] K. Berkelman,[20] D. G. Cassel,[20] J. E. Duboscq,[20] K. M. Ecklund,[20] R. Ehrlich,[20] L. Fields,[20] R. S. Galik,[20] L. Gibbons,[20] B. Gittelman,[20] R. Gray,[20] S. W. Gray,[20] D. L. Hartill,[20] B. K. Heltsley,[20] D. Hertz,[20] L. Hsu,[20] C. D. Jones,[20] J. Kandaswamy,[20] D. L. Kreinick,[20] V. E. Kuznetsov,[20] H. Mahlke-Krüger,[20] T. O. Meyer,[20] P. U. E. Onyisi,[20] J. R. Patterson,[20] D. Peterson,[20] J. Pivarski,[20] D. Riley,[20] J. L. Rosner,[20,†] A. Ryd,[20] A. J. Sadoff,[20] H. Schwarthoff,[20] M. R. Shepherd,[20] W. M. Sun,[20] J. G. Thayer,[20] D. Urner,[20] T. Wilksen,[20] and M. Weinberger[20]

(CLEO Collaboration)

[1] *University of Florida, Gainesville, Florida 32611*
[2] *George Mason University, Fairfax, Virginia 22030*
[3] *University of Illinois, Urbana-Champaign, Illinois 61801*
[4] *Carleton University, Ottawa, Ontario, Canada K1S 5B6 and the Institute of Particle Physics, Canada*
[5] *University of Kansas, Lawrence, Kansas 66045*
[6] *University of Minnesota, Minneapolis, Minnesota 55455*
[7] *Northwestern University, Evanston, Illinois 60208*
[8] *State University of New York at Albany, Albany, New York 12222*
[9] *University of Oklahoma, Norman, Oklahoma 73019*
[10] *University of Pittsburgh, Pittsburgh, Pennsylvania 15260*
[11] *University of Puerto Rico, Mayaguez, Puerto Rico 00681*
[12] *Purdue University, West Lafayette, Indiana 47907*
[13] *Rensselaer Polytechnic Institute, Troy, New York 12180*
[14] *University of Rochester, Rochester, New York 14627*
[15] *Southern Methodist University, Dallas, Texas 75275*
[16] *Syracuse University, Syracuse, New York 13244*
[17] *Vanderbilt University, Nashville, Tennessee 37235*
[18] *Wayne State University, Detroit, Michigan 48202*
[19] *Carnegie Mellon University, Pittsburgh, Pennsylvania 15213*

[20]*Cornell University, Ithaca, New York 14853*

(Dated: August 5, 2004)

Abstract

We have studied the inclusive photon spectrum in $\psi(2S)$ decays using the CLEO III detector. We present the most precise measurements of electric dipole (E1) photon transition rates for $\psi(2S) \to \gamma\chi_{cJ}(1P)$ $(J = 0, 1, 2)$. We also confirm the hindered magnetic dipole (M1) transition, $\psi(2S) \to \gamma\eta_c(1S)$. However, the direct M1 transition $\psi(2S) \to \gamma\eta_c(2S)$ observed by the Crystal Ball as a narrow peak at a photon energy of 91 MeV is not found in our data.

PACS numbers: 14.40.Gx, 13.20.Gd

*Submitted to the 32$^{\text{nd}}$ International Conference on High Energy Physics, Aug 2004, Beijing

†On leave of absence from University of Chicago.

Observation of the triplet of $\chi_{cJ}(1P)$ states ($J = 0, 1, 2$) via radiative E1 transitions from $\psi(2S)$ [1] confirmed the interpretation of the $J/\psi(1S)$ and $\psi(2S)$ states as non-relativistic bound states of a heavy quark-antiquark system and solidified the quark model of hadrons. The best exploration of the inclusive photon spectrum in $\psi(2S)$ decays was achieved by the Crystal Ball experiment two decades ago [2]. The Crystal Ball also claimed observation of two singlet states, $\eta_c(1S)$ and $\eta_c(2S)$ via rare M1 photon transitions [2, 3]. Although many other experiments [4] have confirmed the $\eta_c(1S)$ state, the Crystal Ball $\eta_c(2S)$ candidate remains the sole evidence for this latter state at a mass of 3592 MeV corresponding to a photon energy of 91 MeV. Searches for it in $\bar{p}p$ formation have been unsuccessful [5]. Moreover, the validity of the Crystal Ball $\eta_c(2S)$ candidate has been put in serious doubt by the Belle experiment, which found evidence for the $\eta_c(2S)$ state at a significantly higher mass [6], later confirmed by the CLEO and BaBar experiments [7, 8].

In this paper we present an investigation of the inclusive photon spectrum in the $1.6 \cdot 10^6$ $\psi(2S)$ decays collected with the CLEO III detector, which is comparable in number of resonant decays to the Crystal Ball sample. The CLEO III detector is equipped with an CsI(Tl) calorimeter, first installed in the CLEO II detector [9]. The energy resolution matches the resolution achieved in the Crystal Ball detector. The finer segmentation of the CLEO calorimeter provides for better photon detection efficiency and more effective suppression of the photon background from π^0 decays. The CLEO III tracking detector, consisting of a silicon strip detector and a large drift chamber [10], provides improved suppression of backgrounds from charged particles. The magnetic field inside the tracking detector was 1 T.

The data used in this analysis were collected at the CESR e^+e^- storage ring. CESR has operated for over two decades at the $b\bar{b}$ threshold energy region. Recently, CESR has been reconfigured to run near the $c\bar{c}$ threshold by insertion of 12 superconducting wiggler magnets. The data analyzed in this article come from the first stage of this upgrade in which the first superconducting wiggler magnet was installed. The achieved instantaneous peak luminosity reached $2 \cdot 10^{31}$ cm^{-2}s^{-1}. The integrated luminosity collected and analyzed at the $\psi(2S)$ peak region was 2.7 pb^{-1}.

The data analysis starts with the selection of hadronic events detected at the $\psi(2S)$ resonance. We require that the observed number of charged tracks (N_{ch}) be at least one. The visible energy of tracks and photons (E_{vis}) must be at least 20% (40% if $N_{ch} = 1$) of the center-of-mass energy (E_{CM}). For $1 \leq N_{ch} \leq 3$ the total energy visible in the calorimeter alone (E_{cal}) must be at least 15% of E_{CM}. To suppress $e^+e^- \to e^+e^-$ and $e^+e^- \to \mu^+\mu^-$ events, the momentum of the second most energetic track in the event must be less than 85% of the beam energy, and $E_{cal} < 0.85\,E_{CM}$ for $N_{ch} \leq 3$. We also veto events with invariant mass of e^+e^- or $\mu^+\mu^-$ within 100 MeV of the $J/\psi(1S)$ mass to avoid statistical correlations between this analysis and our studies of the two-photon cascades in $\gamma\gamma l^+l^-$ events. The lepton pair candidates are selected using energy deposited in the calorimeter. The resulting event selection efficiency is 84% for decays of the $\psi(2S)$ resonance.

In the next step of the data analysis we select photon candidates. Showers in the calorimeter are required not to match the projected trajectory of any charged particle, and to have lateral shower profile consistent with that of an isolated electromagnetic shower. We restrict the photon candidates to be within the central barrel part of the calorimeter ($|\cos\theta| < 0.8$) where the photon energy resolution is optimal. The main photon background in this analysis comes from π^0 decays. We can reduce this background by removing photon candidates that combine with another photon to fit the π^0 mass within the experimental resolution.

Unfortunately, this lowers the signal efficiency, since random photon combinations sometime fall within the π^0 mass window. The number of random matches to the π^0 hypothesis can be decreased by restricting the opening angle between the two photons ($\theta_{\gamma\gamma}$). Fig. shows photon energy spectra obtained with various levels of π^0 suppression. We choose the cut $\cos\theta_{\gamma\gamma} > 0.5$ to optimize the statistical sensitivity in the widest range of photon energies.

Fig. 2 shows the fit to the three dominant E1 photon lines $\psi(2S) \to \gamma\chi_{cJ}(1P)$ $(J = 2, 1, 0)$. Each photon line is represented by a convolution of a non-relativistic Breit-Wigner and a detector response function. The latter is parametrized by the so-called Crystal Ball line shape, which is a Gaussian (described by the peak energy, E_p, and energy resolution, σ_E) turning into a power law tail, $1/(E_p - E + const)^n$, at an energy of $E_p - \alpha\,\sigma_E$. This asymmetric low-energy tail is induced by the transverse and longitudinal shower energy leakage out of the group of crystals used in the photon energy algorithm. We determine the parameters describing the leakage tail, n and α, from the fit to $\psi(2S) \to \gamma\chi_{cJ}(1P)$ photon lines observed with essentially no background in $\gamma\gamma l^+l^-$ events (produced via subsequent $\chi_{cJ}(1P) \to \gamma J/\psi(1S)$, $J/\psi(1S) \to l^+l^-$ decays). The natural widths of the $\chi_{cJ}(1P)$ states are fixed to their world average values [4]. Energy resolution parameters, σ_E, are allowed to float. The energy resolution dominates over the natural widths, although the contribution of the natural width is quite significant for the $J = 0$ line. Averaging over the three fitted peaks and using the photon energy dependence predicted by the Monte Carlo, we get a fitted photon energy resolution (extrapolated to $E_\gamma = 100$ MeV) of 4.8 ± 0.3 MeV, where the error is systematic. We represent the photon background under the peaks by a 4^{th} order polynomial. We include also the charged particle energy distribution measured for photon candidates matched to charged tracks, with the track-match-miss probability fixed to the expected value (1%). The peaking of this distribution around 200 MeV comes from minimum ionizing tracks. We also include in the fit a small Doppler broadened photon line at 115 MeV due to $\psi(2S) \to XJ/\psi(1S)$, $J/\psi(1S) \to \gamma\eta_c(1S)$ with the amplitude fixed to the number estimated using the world average branching ratios [4].

The fitted number of events, with photon line energies and statistical errors are $79\,300 \pm 1\,180$ (128.00 ± 0.08 MeV), $76\,700 \pm 910$ (172.05 ± 0.08 MeV) and $72\,630 \pm 930$ (261.99 ± 0.14 MeV) for $\psi(2S) \to \gamma\chi_{cJ}(1P)$ $J = 2$, 1 and 0, respectively.

To estimate systematic errors on the fitted photon energies we vary the fitted range, the order of the background polynomial, the detector response parameters (α and n), the normalization of the charged particle spectrum, the natural widths of $\chi_{cJ}(1P)$ states; and we use linear rather than logarithmic binning in energy. We also vary the level of π^0 suppression from no suppression to $\cos\theta_{\gamma\gamma} > 0.3$ (see Fig.). The corresponding systematic errors on the photon energies are $\pm 0.08\%$, $\pm 0.10\%$ and $\pm 0.13\%$ for $J = 2$, 1 and 0 respectively. There is also a common energy scale error of $\pm 0.5\%$, due the systematic limitation of the calibration procedure based on π^0 and η masses [11]. Adding the statistical and uncorrelated systematic errors together (the first error) and factoring out the energy scale error (the second error), we get the following measured photon energies: $(128.00 \pm 0.13 \pm 0.64)$ MeV, $(172.05 \pm 0.19 \pm 0.86)$ MeV, and $(261.99 \pm 0.37 \pm 1.31)$ MeV for $J = 2$, 1 and 0 respectively, in good agreement with the masses of the $\psi(2S)$ and $\chi_{cJ}(1P)$ states precisely measured via scans of these resonances [4]. A ratio of the fine mass splitting in the $\chi_{cJ}(1P)$ triplet determined from our photon energy measurements is: $r \equiv (M(\chi_{c2}) - M(\chi_{c1}))/(M(\chi_{c1}) - M(\chi_{c0})) = 0.490 \pm 0.002 \pm 0.003$.

The fitted peak amplitudes serve for the determination of the photon transition branching ratios. We determine signal selection efficiencies by Monte Carlo simulation to be $54\%, 54\%$ and 50% for $J = 2, 1$ and 0, including factors due to spin-dependent $\cos\theta$ distributions.

To obtain branching ratios, we divide the efficiency-corrected photon yields by the number of $\psi(2S)$ resonances produced. The latter is determined by background-subtracted and efficiency-corrected yield of hadronic events in our data. To estimate systematic uncertainty, hadronic event selection criteria are varied, resulting in a $\psi(2S)$ efficiency change from 58% to 87%. Cosmic ray, beam-gas and beam-wall backgrounds vary from 0.1% to 3.3% as estimated from the tails of the event vertex distribution along the beam direction. The QED backgrounds ($e^+e^- \to e^+e^-$, $e^+e^- \to \mu^+\mu^-$ and $e^+e^- \to \tau^+\tau^-$) are estimated using the Monte Carlo simulations normalized to theoretically calculated cross-sections [12] and measured integrated luminosity. The Bhabha scattering background varies from 0 to 2%, while the $\mu-$pair and $\tau-$pair backgrounds do not exceed 0.3%. Continuum production of hadrons amounts to a $2.4-2.6\%$ background subtraction and is estimated using the Monte Carlo simulation normalized to the continuum cross-section measured by the other experiments [4]. Uncertainties in modeling of decays of $c\bar{c}$ states partially cancel between the signal and hadronic selection efficiencies. The overall systematic error in the branching ratio normalization is $\pm 3\%$. The other systematic errors on the branching ratios are determined by the photon selection and fit variations described previously. Electromagnetic shower simulations contributes additional $\pm 2\%$.

Our $\mathcal{B}(\psi(2S) \to \gamma\chi_{cJ}(1P))$ results are $(9.33 \pm 0.14 \pm 0.61)\%$, $(9.07 \pm 0.11 \pm 0.54)\%$, and $(9.22 \pm 0.11 \pm 0.46)\%$ for $J = 2$, 1 and 0 respectively. They are significantly higher than values obtained by the Particle Data Group by a global fit to the $\psi(2S)$ data [4], but agree well with the previous measurements by the Crystal Ball [2], ($8.0 \pm 0.5 \pm 0.7$, $9.0 \pm 0.5 \pm 0.7$ and $9.9 \pm 0.5 \pm 0.8$ % respectively), and have improved statistical and systematic errors. Since the statistical and systematic errors are partially correlated for the three $\chi_{cJ}(1P)$ states we also provide a sum and ratios of these branching ratios with properly evaluated errors: $\mathcal{B}(\psi(2S) \to \gamma\chi_{c0,1,2})(1P) = (27.6 \pm 0.3 \pm 2.0)\%$, $\mathcal{B}(\psi(2S) \to \gamma\chi_{c2}(1P))/\mathcal{B}(\psi(2S) \to \gamma\chi_{c1}(1P)) = 1.03 \pm 0.02 \pm 0.03$, $\mathcal{B}(\psi(2S) \to \gamma\chi_{c0}(1P))/\mathcal{B}(\psi(2S) \to \gamma\chi_{c1}(1P)) = 1.02 \pm 0.01 \pm 0.07$ and $\mathcal{B}(\psi(2S) \to \gamma\chi_{c0}(1P))/\mathcal{B}(\psi(2S) \to \gamma\chi_{c2}(1P)) = 0.99 \pm 0.02 \pm 0.08$.

In addition to the dominant E1 photon peaks, we also observe a small peak at higher photon energy due to the hindered M1 transition $\psi(2S) \to \gamma\eta_c(1S)$. The fit, illustrated in Fig. 3, of Breit-Wigner convoluted with the Crystal Ball line shape yields $2\,560 \pm 315$ events (with a statistical significance of 8.1 standard deviations) and a transition photon energy of $(646.2 \pm 2.6 \pm 4.8)$ MeV, where the first error is statistical and the second error is systematic. The measured photon energy is within $(1.2 \pm 0.9)\%$ of the expected value determined from the world average masses of the $\psi(2S)$ and $\eta_c(1S)$ states [13].

The detection efficiency is 51% for these transitions. The fitted peak amplitude depends strongly on the assumed natural width of the $\eta_c(1S)$. In our nominal fit we assumed $\Gamma_{\eta_c(1S)} = 24.8 \pm 4.9$ MeV, coming from our own determination via formation in $\gamma\gamma$ collisions [7]. When left free in the fit, the fitted width is consistent with this value. Since the exact value of this width is a subject of experimental controversy [13], we factor the $\Gamma_{\eta_c(1S)}$ dependence out to enable a rescaling of our results to a different value in the future. The central value of the branching ratio ($\mathcal{B}$) can be expressed as

$$\mathcal{B} = \left(0.324 + 0.028\,\frac{\Gamma_{\eta_c(1S)} - 24.8\mathrm{MeV}}{4.9\mathrm{MeV}}\right) \quad \%$$

and the errors are

$$(\pm 0.039 \pm 0.055)\,\frac{\mathcal{B}}{0.324\%} \quad \pm \left(0.028\,\frac{\Delta\Gamma_{\eta_c(1S)}}{4.9\mathrm{MeV}}\right) \quad \%.$$

The first error is statistical, the second is systematic, and the third is due to the uncertainty in the $\Gamma_{\eta_c(1S)}$ width. For our nominal choice of $\Gamma_{\eta_c(1S)}$ and $\Delta\Gamma_{\eta_c(1S)}$ we obtain $\mathcal{B}(\psi(2S) \to \gamma\eta_c(1S)) = (0.32 \pm 0.04 \pm 0.06)\%$. The first error is statistical and the second is the total systematic uncertainty. This is the first confirmation of this transition, previously detected by the Crystal Ball. The Crystal Ball measured the rate for this transition to be $(0.28 \pm 0.06)\%$ for $\Gamma_{\eta_c(1S)} = (11.5 \pm 4.5)$ MeV [2]. Rescaled to this width, our result, $(0.25 \pm 0.06)\%$, is in good agreement with their measurement.

The Crystal Ball also presented evidence for the direct [3] M1 transition $\psi(2S) \to \gamma\eta_c(2S)$ with $E_\gamma = (91 \pm 5)$ MeV, $\mathcal{B}(\psi(2S) \to \gamma\eta_c(2S)) = (0.2 - 1.3)\%$ at 95% confidence level (C.L.) and $\Gamma_{\eta_c(2S)} < 8$ MeV at 95% C.L. We see no evidence for such a photon line (see Fig. 2) and set an upper limit for the transition rate to a $\Gamma = 8$ MeV state at this photon energy to be $< 0.2\%$ at 90% C.L.

Recent observations of the $\eta_c(2S)$ state [13] imply the photon energy for such a transition to be about 47 MeV with a larger width. Since a small and wide photon line at such low photon energy cannot be distinguished from the photon backgrounds (for example, the width of such a peak for $\Gamma_{\eta_c(2S)} = 25$ MeV would be about 12 times broader in Fig. than the width of the first E1 line), we have no meaningful sensitivity for such a transition at the new $\eta_c(2S)$ mass.

In summary, we have improved branching ratio measurements for $\psi(2S) \to \gamma\chi_{c0,1,2}(1P)$ (E1 transitions) and $\psi(2S) \to \gamma\eta_c(1S)$ (hindered M1 transitions). The latter is the first confirmation of the existence of such a transition. The direct M1 transition $\psi(2S) \to \gamma\eta_c(2S)$ is not observed and the upper limit is set below the branching ratio range previously claimed by the Crystal Ball experiment [3].

We gratefully acknowledge the efforts of the CESR staff in providing us with excellent luminosity and running conditions. This work was supported by the National Science Foundation, the U.S. Department of Energy, the Research Corporation, and the Texas Advanced Research Program.

---

[1] J.S. Whitaker *et al.*, Phys. Rev. Lett. **37** 1596 (1976); C.J. Biddick *et al.*, Phys. Rev. Lett. **38**, 1324 (1977).
[2] Crystal Ball Collaboration, J.E. Gaiser *et al.* , Phys. Rev. D **34**, 711 (1986).
[3] Crystal Ball Collaboration, C. Edwards *et al.*, Phys. Rev. Lett. **48**, 70 (1982).
[4] PDG Collaboration, S. Eidelman *et al.* Phys. Lett. B **592**, 1 (2004).
[5] E835 Collaboration, M. Ambrogiani *et al.*, Phys. Rev. D **64**, 052003 (2001).
[6] BELLE Collaboration, S.K. Choi *et al.*, Phys. Rev. Lett. **89**, 102001 (2002), Erratum-ibid. **89**, 129901 (2002). K. Abe *et al.*, Phys. Rev. Lett. **89**, 142001 (2002).
[7] CLEO Collaboration, D.M. Asner *et al.*, Phys. Rev. Lett. **92**, 142001 (2004).
[8] BaBar Collaboration, B. Aubert *et al.*, Phys. Rev. Lett. **92**, 142002 (2004).
[9] CLEO Collaboration, Y. Kubota *et al.*, Nucl. Instr. Meth. A **320**, 66 (1992).
[10] D. Peterson *et al.*, Nucl. Instr. Meth. A **478**, 142 (2002).
[11] CLEO Collaboration, R. Morrison *et al.*, Phys. Rev. Lett. **67**, 1696 (1991).
[12] S. Jadach, E. Richter-Was, B.F.L. Ward, Z. Was, Comput. Phys. Commun. **70** 305 (1992); R. Kleiss, S. van der Marck, Nucl. Phys. B **342**, 61 (1990); S. Jadach, Z. Was, Comput. Phys. Commun. **85**, 453 (1995).

[13] For a compilation of old and new measurements of $\eta_c(1S)$ and $\eta_c(2S)$ masses and widths see T. Skwarnicki, Int. J. Mod. Phys. A **19**, 1030 (2004).

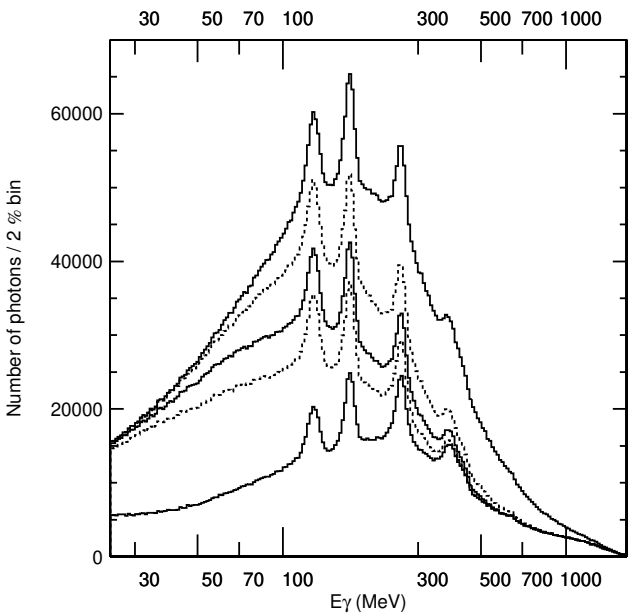

FIG. 1: Going from bottom to top, the histograms show the photon energy spectra at the $\psi(2S)$ resonance omitting those photons which, with another photon in the event, form a π^0 candidate with $\cos\theta_{\gamma\gamma}$ exceeding: -1; i.e. maximal π^0 suppression (solid), 0.3 (dashed), 0.5 (solid), 0.7 (dashed), 1.0; i.e. no π^0 suppression (solid).

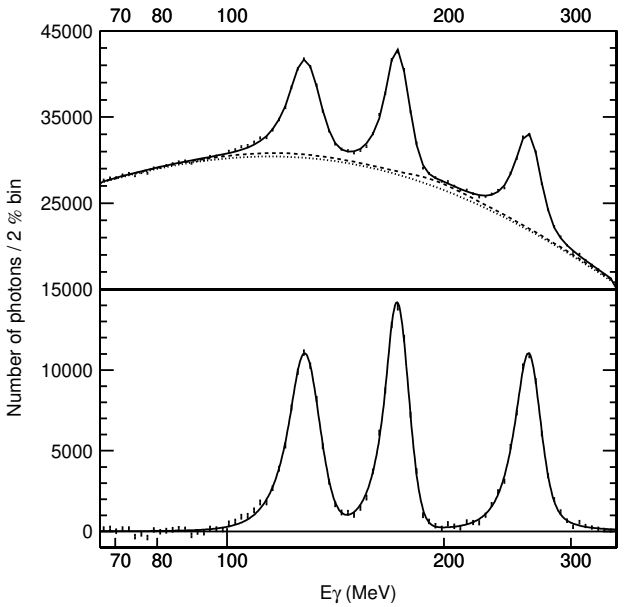

FIG. 2: Fit of $\psi(2S) \to \gamma\chi_{cJ}(1P)$ $(J = 2, 1, 0)$ photon lines to the data. The points with error bars represent the data. The solid line represents the fit. The dashed line represents total fitted background. The dotted line represents the polynomial background alone, without the contributions from charged particles and the decays $J/\psi(1S) \to \gamma\eta_c(1S)$. The background subtracted data (points with error bars) and the fitted photon lines superimposed (solid line) are shown at the bottom.

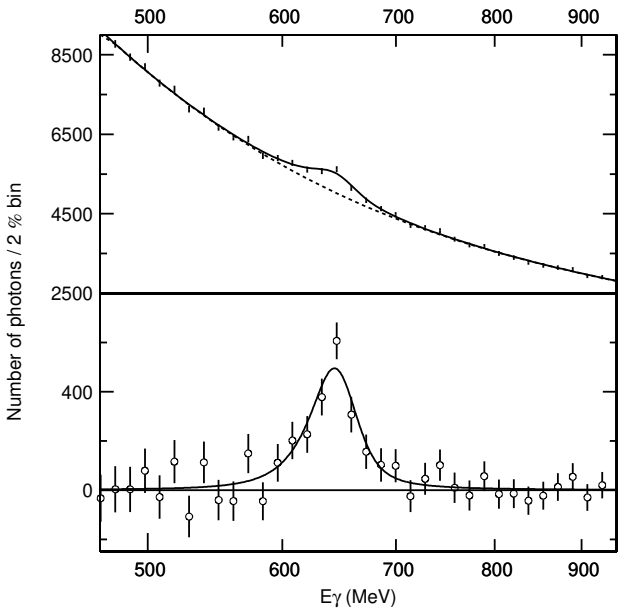

FIG. 3: Fit of $\psi(2S) \to \gamma\eta_c(1S)$ photon line to the data. The points with error bars represent the data. The solid line represents the fit. The dashed line represents total fitted background. The background subtracted data (points with error bars) and the fitted photon line superimposed (solid line) are shown at the bottom.